Effect of Skin Indentation on Heat Transfer During Cryogen Spray Cooling

Brooke Basinger, BS,[1] Guillermo Aguilar, PhD,[1,2]* and J. Stuart Nelson, MD, PhD[1]
[1]*Beckman Laser Institute, University of California, Irvine, California 92612*
[2]*Department of Mechanical Engineering, University of California, Riverside, California 92521*

Background and Objectives: Cryogen spray cooling (CSC) is used to pre-cool the epidermis during dermatological laser procedures such as treatment of port wine stain (PWS) birthmarks, hair removal, and non-ablative photorejuvenation. Thus far, heat transfer studies related to CSC optimization have assumed a flat surface but clinical observation suggests that human skin indents due to the force of an impinging cryogen spray.
Study Design/Materials and Methods: High-speed videos of cryogen spray impingement on in vivo human skin were taken and the resulting indentations characterized as a function of both nozzle-to-skin distance and anatomic location. Detectors with pre-formed indentations were constructed and heat flux measurements were performed at two nozzle-to-surface distances.
Results: Indentation causes cryogen accumulation that reduces the efficiency of heat transfer when compared to spray impingement on a flat surface. Large indentations, however, encourage convective flow within the cryogen pool that mitigates many of the negative effects of liquid layer thickening and improves the heat flux.
Conclusions: Flat surfaces produce the most efficient heat transfer, but once indentation exists (as it does in all clinically relevant cases), larger indentations produce a higher maximum heat flux. This suggests that higher momentum sprays (which produce larger skin indentations for identical spurts) than those in current clinical use may improve CSC efficiency. Lasers Surg. Med. 34:155–163, 2004.

Key words: heat transfer; cryogen spray cooling; skin indentation

INTRODUCTION

Laser therapy is an effective method for treatment of port wine stain (PWS) birthmarks [1], hair removal [2], and non-ablative photorejuvenation [3]. Although these therapies target chromophores in the dermis, absorption of laser energy by epidermal melanin causes localized heating therein and increases the risk of non-specific thermal damage [1,4], thereby limiting the maximal radiant exposure that can be safely used clinically.

Cryogen spray cooling (CSC) selectively pre-cools the epidermis without reducing the temperature of deeper targets [5]. To obtain optimal cooling selectivity, particularly for shallow targets such as PWS and patients with high melanin concentrations (e.g., skin types $\geq$ III), it is important to understand, control and maximize heat transfer occurring between the cryogen spray and skin surface.

The effects of spray characteristics [6], nozzle-to-skin distance [7,8], and spurt duration [9] on heat transfer have been investigated in attempts to optimize CSC parameters. These studies were performed using flat, non-deformable surfaces as spray targets and temperature measurement devices [10–15]. However, clinical observation during CSC suggests that human skin deforms due the momentum of the spray, creating an indentation that affects the mechanics of spray impingement and deposition and, therefore, must affect heat transfer as well.

This study investigates skin indentation that occurs during CSC and its effect on heat transfer. High-speed videos of spray impingement on in vivo human skin were used to characterize indentation under a variety of spray conditions. Custom-made heat flux sensors with pre-formed concave surfaces approximating those observed in human skin were designed to study the effects of indentation on heat transfer.

EXPERIMENTAL METHODS AND PROCEDURES

Cryogen Delivery and Nozzles

The cryogen used in this study is 1,1,1,2 tetrafluoroethane, also known as R-134a, with boiling temperature $T_b \approx -26^\circ$C at atmospheric pressure. Liquid cryogen is kept in a metal container at saturation pressure (660 kPa at 25°C), and delivered through a high-pressure rubber hose to an electronically controlled fuel injector attached to straight-tube nozzles. The nozzles are made of stainless steel with inner diameter, d_N, of 0.7 mm and lengths, l_N, of 31.8 and 63.6 mm, respectively, soldered to a custom-made copper coupling which fitted tightly around the fuel injector. The nozzle with $l_N = 31.8$ mm, similar in both diameter and length to those used in commercial devices,

Contract grant sponsor: National Institutes of Health (to JSN); Contract grant numbers: GM-62177, AR-47551; Contract grant sponsor: National Institutes of Health (to GA); Contract grant number: HD-42057.
*Correspondence to: Guillermo Aguilar, PhD, Department of Mechanical Engineering, University of California, Riverside, CA 92521. E-mail: gaguilar@engr.ucr.edu
Accepted 3 December 2003
Published online in Wiley InterScience (www.interscience.wiley.com).
DOI 10.1002/lsm.20011

was used for in vivo spray impingement studies. Previous work by our group [15] showed that this nozzle exhibits spray parameters and heat flux characteristics very similar to commercially available GentleLASE^{TM}, Smoothbeam^{TM}, Vbeam^{TM}, and CBeam^{TM} nozzles. Heat transfer measurements were performed using a nozzle with $l_N = 63.6$ mm, shown to have a transition region between nozzle-to-surface distances (z) of 25 and 30 mm, where spray characteristics are likely to have large variations [16]. Therefore, we chose one z on either side of the transition region (20 and 40 mm) for these studies.

Imaging System

A high speed camera (Photron Fastcam PCI 10K, Itronics, Westlake Village, CA) with a 90 mm zoom lens (V-HQ Macro MC 90 mm f/2.5, Elicar, Japan) was used to acquire digital images of spray impingement on in vivo human skin. Image sequences were captured at a rate of 500 frames per second and pixel resolution of 512×240. The target skin surface was colored black using a non-toxic erasable marker to improve image contrast.

Image Analysis

Measuring skin surface indentation directly during droplet impingement without interfering with the spray was prohibitively complex. Instead, indentation depths resulting from spray impingement were calculated from the digital video image. A schematic of the digital video apparatus and skin indentation analysis is shown in Figure 1.

In a previous study [15], it was determined that sprays resulting from nozzles similar to those used herein are radially symmetrical. It may, therefore, be assumed that the skin indentation resulting from such a spray is also radially symmetrical. In that case, the exact angle of the camera for any given image sequence can be found using Equation 1, where θ is the angle between the camera and surface being sprayed, D_h is the horizontal diameter, in pixels, of the indentation noted in the video image and D_v is the vertical diameter seen in the image (which has been foreshortened as a result of the camera angle).

$$\sin\theta = \frac{D_v}{D_h}. \tag{1}$$

Similarly, the indentation depth observed in the image can then be adjusted to eliminate the foreshortening effect using Equation 2, where d_{image} is the distance observed in the video between the original skin position and that after indentation and d_{actual} is the corrected distance.

$$\cos\theta = \frac{d_{image}}{d_{actual}}. \tag{2}$$

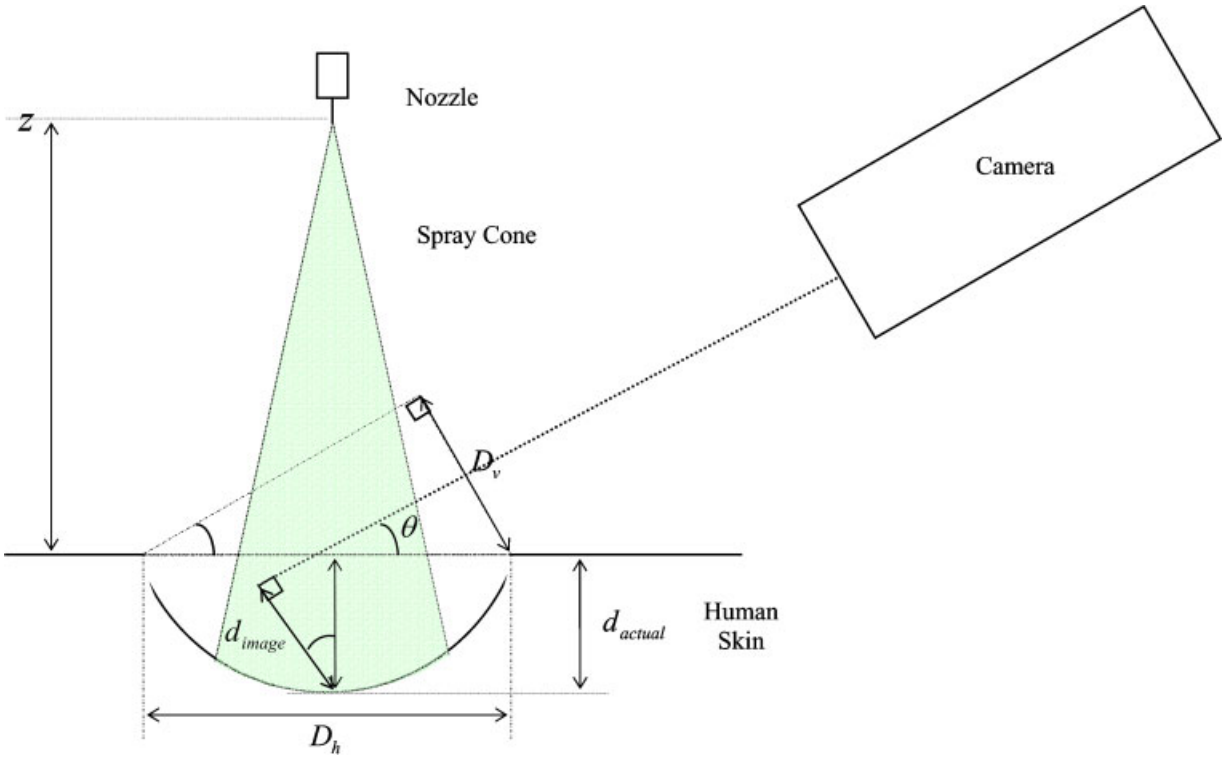

Fig. 1. Schematic of digital video apparatus and skin indentation analysis. Distances perceived by the camera (those that are perpendicular to the path of the camera) are foreshortened as a result of the angle, θ, and must be corrected to find the actual depth of indentation in the skin during cryogen spray cooling (CSC).

For every image sequence, the scale relating pixel size to physical distance was noted and all measurements adjusted accordingly.

With this method, the indentation depth can be measured at any given point on the skin surface, allowing a profile to be created. However, the method is limited by image clarity and resolution and depends on the ability of the individual observer to determine visually the indentation edges. Based on camera resolution and typical image quality, we estimate the accuracy of this method to be ± 0.2 mm.

Temperature Measurement Sensors

Heat flux sensors with different pre-formed indentations were designed and built using a model previously developed by Aguilar et al. [16]. Each sensor consisted of a miniature type-K thermocouple ($\sim$250 μm bead diameter) soldered to a thin (90 μm) layer of silver foil, approximately 3 by 3 mm, and encased on one side in an epoxy block with thermal properties similar to those of human skin [16]. The small metallic foil coupled with miniature sensors provides fast, dynamic surface temperature measurements while the embedding epoxy provides a thermal environment similar to that of human skin. Overall heat extraction, Q, and surface heat flux, q, are of the same order of magnitude as those expected for human skin. Published thermal properties of the materials used to build these sensors are shown in Table 1 [17,18]. Thermal properties of human dermis [19] are also given for reference. The pieces of silver foil differed in volume and thus specific heat capacity by no more than 4%.

Each sensor was constructed using a Teflon mold with a semispherical protrusion of known depth and radius of curvature, R_c, as shown in Figure 2. The silver foil was fitted to the protrusion and liquid epoxy poured into the mold, eventually producing static, semispherical indentations in the epoxy with R_c of either 9.52 or 6.34 mm and depths, d, ranging from 0.96 to 3.33 mm. Care was taken that the silver foil remained at the deepest point (center) of the indentation and that the opening was wide enough to encompass fully the spray cone (i.e., no cryogen impacted the sensor outside the indentation). One flat control sensor without indentation was constructed using the same method. Relevant design values for each sensor are shown in Table 2.

All thermocouple measurements are acquired at 2 kHz and converted to temperature data using a dedicated data acquisition system with an added thermocouple module (SCXI-1000, SCXI-1303, National Instruments, Austin, TX), managed by a custom program written in LabView 6.1. This acquisition rate ensured an appropriate resolution given the sensor thermal response time which, considering the size and geometry of the materials used and average cooling conditions to which it was exposed, we estimate to be on the order of 5–8 milliseconds. The sensor was allowed to return to ambient temperature between each experiment.

Mathematical Model and Inverse Heat Transfer Algorithm

CSC dynamics can be simplified to a one-dimensional heat conduction problem if uniform heat transfer over the sprayed surface is assumed, in which an Inverse Heat Conduction Problem (IHCP) algorithm can be employed. We used the Sequential Function Specification Method (SFSM) of Beck et al. [20], which estimates q as a piecewise constant function of time at each time step. This method has been previously employed in similar studies [9,21] and a more detailed discussion of its application to CSC can be found in Tunnell et al. [21].

RESULTS

Skin Indentation During CSC

A typical video frame of spray impingement on in vivo human skin, 30 milliseconds after initial droplet impact, with $z = 30$ mm, is seen in Figure 3. Cryogen spray can be seen entering the frame from above and impacting the blackened (for contrast) human skin. The indentation created by the force of the spray is readily apparent.

In Figure 4, indentations observed during spray impingement for several different z and anatomic locations are systematically quantified as described above. Figure 4a shows the indentations observed when spraying the dorsal side of an open hand held as flat as possible underneath the nozzle, with $z = 15$, 20, 30, 40, and 50 mm. Those indentations observed when spraying various anatomic locations (dorsal side of a closed hand, dorsal side of an open hand, and volar forearm) with $z = 20$ mm are shown in Figure 4b.

These indentations can be characterized by both d and R_c, but it is impossible to describe fully a given indentation using either number independently. In order to combine the information provided by both d and R_c in a single value, we have chosen to characterize indentations by their

TABLE 1. Thermal Properties of Materials Used in Heat Flux Sensors

Properties	Ag foil	RBC 3100 epoxy	Dermis
Thickness (mm)	0.090	—	—
Thermal conductivity, k (W/(m K))	429	0.217	0.54
Density, ρ (kg/m^3)	10,500	1,160–1,400	1,150
Specific heat, c (J/(kg K))	235	—	3,700
Thermal diffusivity, α_{avg} (m^2/s)	$1{,}739 \times 10^{-7}$	1.22×10^{-7}	1.26×10^{-7}

Human dermal properties are provided for reference.

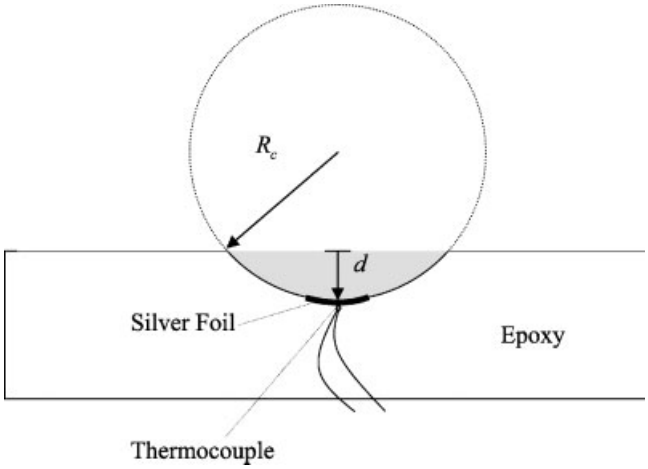

Fig. 2. Schematic of heat flux sensor construction. The shaded area is the cross-sectional area, A_{cs}, of the indentation.

cross-sectional area, A_{cs}, which can be calculated using Equation 3.

$$A_{cs} = \left[\arccos\frac{R_c - d}{R_c}\right]R_c^2 - R_c - d\sqrt{R_c^2 - (R_c - d)^2} \quad (3)$$

A_{cs} is represented by the shaded area in Figure 2. The indentations observed for varying z and anatomic locations are represented as a function of A_{cs} in Figure 5a,b, respectively. In general, observed indentations fall within ranges of $d = 0$–2.9 mm, $R_c = 4$–20 mm, and $A_{cs} = 4$–18 mm^2. Indentations created by cryogen sprays using commercially available nozzles can reasonably be expected to fall within the same ranges, although the exact dimensions of any given indentation will depend on the specific nozzle used, z and anatomic location.

The dynamics of indentation development and recovery after spurt termination were also noted. The indentations observed in this study fully developed during the first 10 milliseconds of the spray, after which they maintained a constant shape throughout the spurt. Following spurt termination, the skin returned to its original shape over a period of time approximately equal to spurt duration for those spurt durations investigated. The A_{cs} observed during 30, 50, and 100 milliseconds spurts on the dorsal open hand are shown in Figure 6 where $z = 40$ mm.

TABLE 2. Relevant Properties of Heat Flux Sensor Indentations

Depth, d (mm)	Radius of curvature, R_c (mm)	Cross-sectional area, A_{cs} (mm^2)
Flat	∞	0
0.96	9.52	5.39
1.78	6.34	10.79
2.44	6.34	17.01
3.12	6.34	24.14
3.33	9.52	33.42

The depths observed in videos of spray impingement on in vivo human skin ranged from 0.20 to 2.79 mm, R_c ranged from ~4 to 20 mm^2, and A_{cs} ranged from ~4 to 18 mm^2.

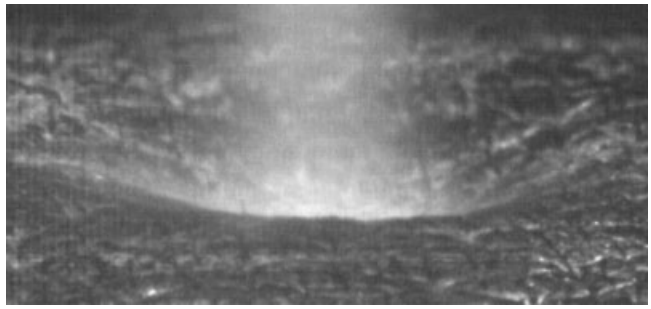

Fig. 3. Typical frame from an in vivo spray impingement video. $z = 30$ mm, which is similar to sprays used during clinical use. Spurt duration was 100 milliseconds, though this frame occurs 30 milliseconds after spray impact.

Heat Transfer

Temperature profiles measured by the flat and each of the curved heat flux sensors during and after a 50 milliseconds spray are shown in Figure 7. Each profile shown is the average of six trials, normalized to begin at a temperature of 20°C. Trials were performed with $z = 20$ and 40 mm. At $z = 20$ mm (Fig. 7a), the temperature of the flat (zero indentation) sensor dropped the quickest and reached the lowest minimum in response to the cryogen spray. Among the curved sensors, that with the smallest A_{cs} (i.e., the smallest indentation overall) responded the slowest and demonstrated the highest minimum temperature. As the A_{cs} of the sensors increased, both the slope of the temperature profile during the first 200 milliseconds and the minimum temperature decreased. Some variation in temperature behavior is seen long after spurt termination, but in the time relevant to dermatologic laser treatments (0–200 milliseconds after spurt onset) the temperature behavior varies regularly with A_{cs}. Sensors with $A_{cs} = 17.01$ and 24.14 mm^2 show the least differentiation from one another, but do follow the overall trend.

At $z = 40$ mm (Fig. 7b), the flat sensor again shows the quickest temperature response and reaches the lowest minimum temperature within the first 200 milliseconds. Again, the curved sensors show a regular variation in temperature behavior with A_{cs}. The speed of the temperature response and minimum temperature reached both "improve" with increasing A_{cs}. Although the time period of interest for shallow target clinical applications is never longer than 200 milliseconds, it should be noted that, at this specific z, all sensors show a tendency to remain at low temperatures long after spurt termination, sometimes even exhibiting a continuous decline in temperature. This trend occurs to some degree in all sensors, but is most notable in those with larger indentations.

The surface heat flux, q, calculated using the IHCP algorithm discussed above is presented for $z = 20$ and 40 mm in Figure 8a,b, respectively. In both z, the flat

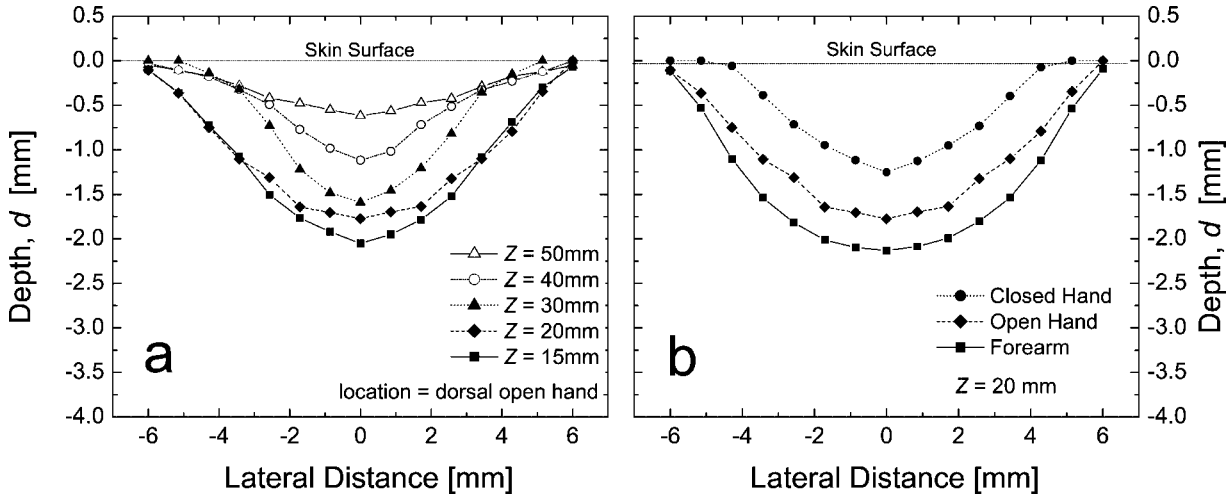

Fig. 4. Indentations observed for varying (**a**) z, where the target is the dorsal side of the open hand, and (**b**) anatomic locations where z is 20 mm.

sensor representing spray impingement with no indentation produces the highest maximum heat flux, q_{max}. The sensor with $A_{cs} = 5.39$ mm^2, representing a reasonably small indentation (and one very similar to those typically produced by commercial nozzles), reaches a q_{max} that is 30% lower than with the flat sensor when $z = 20$ mm, and 28% lower when $z = 40$ mm. As A_{cs} increases, q_{max} also increases.

DISCUSSION

All videos were taken using spray parameters (τ_d and z) and nozzles similar to those used clinically. Indentations occurring in response to the mechanical momentum of impinging droplets were observed and recorded (Fig. 3). As z increases, droplet velocity decreases which yields lower spray momentums and thus smaller indentations (Figs. 4a and 5a). Indentation size also depends on anatomic location (Figs. 4b and 5b) with more pliable locations producing larger indentations. Although nozzles were placed perpendicular to the spray surface in this study, some commercial devices orient the cryogen nozzle at a non-normal incidence angle. Preliminary investigations indicate that this angle may alter the exact shape of skin indentations, but it will not significantly reduce their magnitude. Some commercial devices also employ a distance gauge that circles the treatment area and artificially constrains the spread of the cryogen layer. This will significantly alter the mechanics of spray deposition and may limit the amount of indentation that takes place. This gauge may also confine the area over which the cryogen can spread, inducing a thicker cryogen layer and thus decreasing the cooling efficiency. The complexity of this

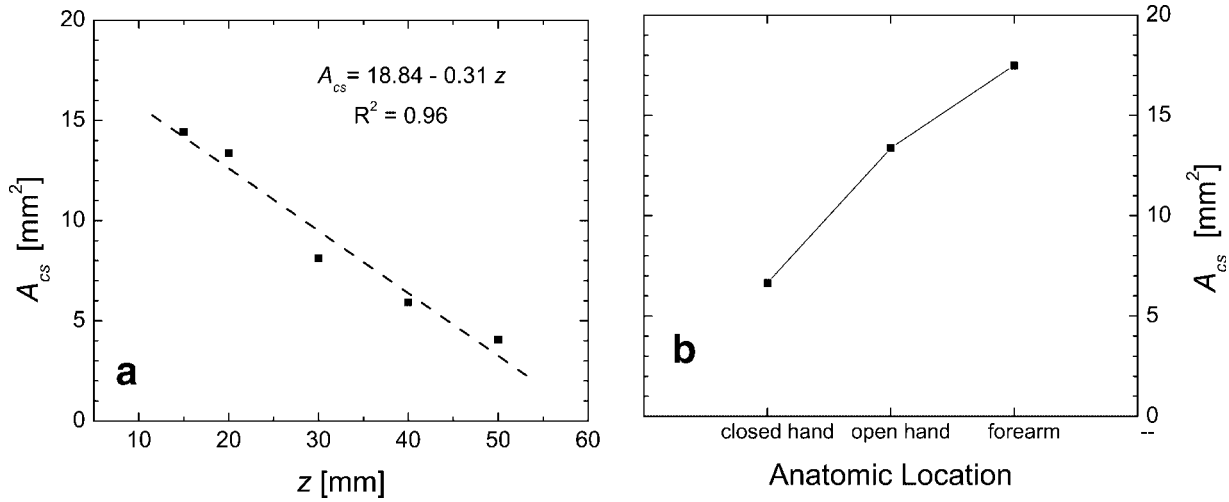

Fig. 5. Indentations, defined in terms of A_{cs}, observed for varying (**a**) z and (**b**) anatomic locations.

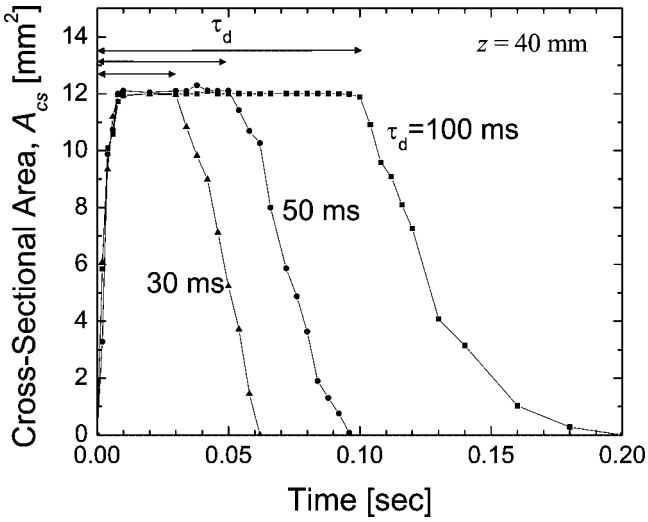

Fig. 6. A_{cs} of indentations observed during and after spray impingement for 30, 50, and 100 milliseconds sprays at $z = 40$ mm. In each case, the indentation forms quickly during the first 10 milliseconds of the spray, then maintains a steady state throughout the spurt before relaxing to $A_{cs} = 0$. Interestingly, the relaxation times are approximately the same as the spurt duration for all three curves. This implies that some indentation in the skin may still exist when laser irradiation occurs.

effect places it beyond the scope of this study but indicates that a study dedicated to the effects of spray angle and distance depth gauges may be warranted.

Although the method used to quantify indentation size is an indirect approach that depends on the individual researcher's ability to define visually the indentation edge, we have judged its accuracy sufficient for this study. Any errors were systematic as the same observer performed all video analyses. The obvious smoothness and regularity of the indentations presented in Figure 4a,b support this assertion. In addition, different patients, anatomic locations and positions during droplet impingement will all affect the indentations created during clinical use. As such, it is impossible to predict the indentation that may occur in a specific situation with complete accuracy and an accuracy of ± 0.2 mm is sufficient for this study. We have investigated skin mechanics due to cryogen spray impingement to determine the range in which such indentations can be expected to occur. Once a range of possible indentations was established, heat flux sensors were built with indentations encompassing that range (Table 2, Figs. 4 and 5).

The skin dynamics shown in Figure 6, indicate that indentations quickly reach a steady state that is then maintained throughout the spurt duration. Although investigating heat flux during the initial 10 milliseconds of the spurt where the indentation is dynamic may prove interesting, indentation stability during the remainder of the spurt justifies our use of pre-indented sensors. Figure 6 also shows that the time for skin to return completely to its original condition is approximately equal to spurt duration for those spurt durations investigated. This suggests that some indentation may still be present when laser irradiation occurs (typically 30–50 milliseconds after spurt termination) during clinical use. Such indentation may negatively affect irradiation uniformity and/or the transmission of laser light through the cryogen layer to the target chromophore, though these topics were beyond the scope of this study.

During spray impingement, cryogen collects within the indentation created in the skin. This causes the formation

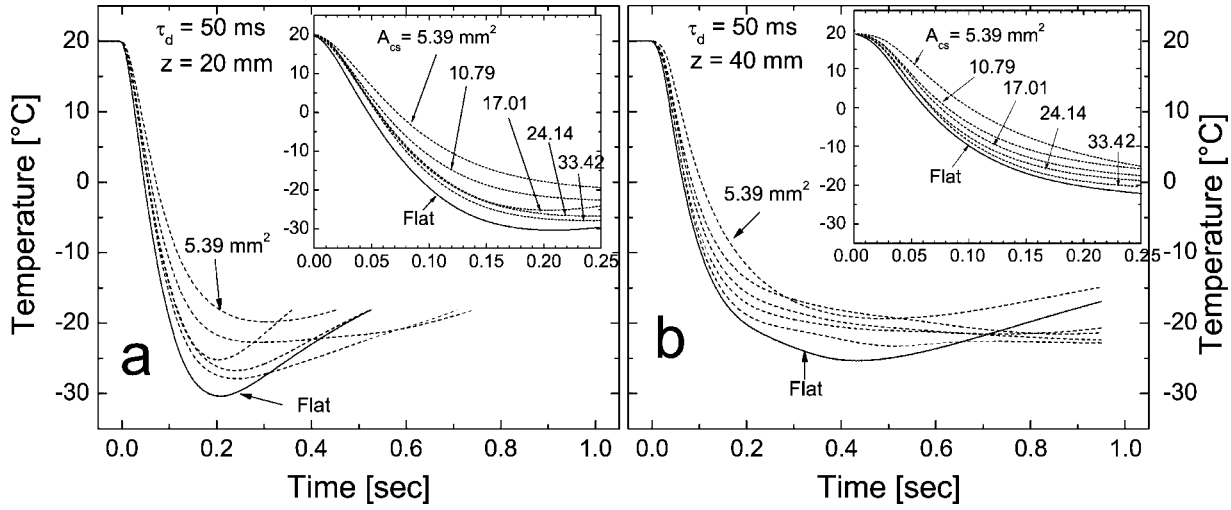

Fig. 7. Temperature as a function of time, measured by heat flux detectors with various pre-formed, static, semispherical indentations. Spurt duration is $\tau_d = 50$ milliseconds, $z = 20$ mm (**a**) and 40 mm (**b**). The first 250 milliseconds after spurt onset is enlarged in the inset window. Sensors are labeled in the inset window according to their A_{cs}. In each case, the slope of the temperature change during the first 200 milliseconds decreases as A_{cs} increases and the flat sensor shows the steepest slope.

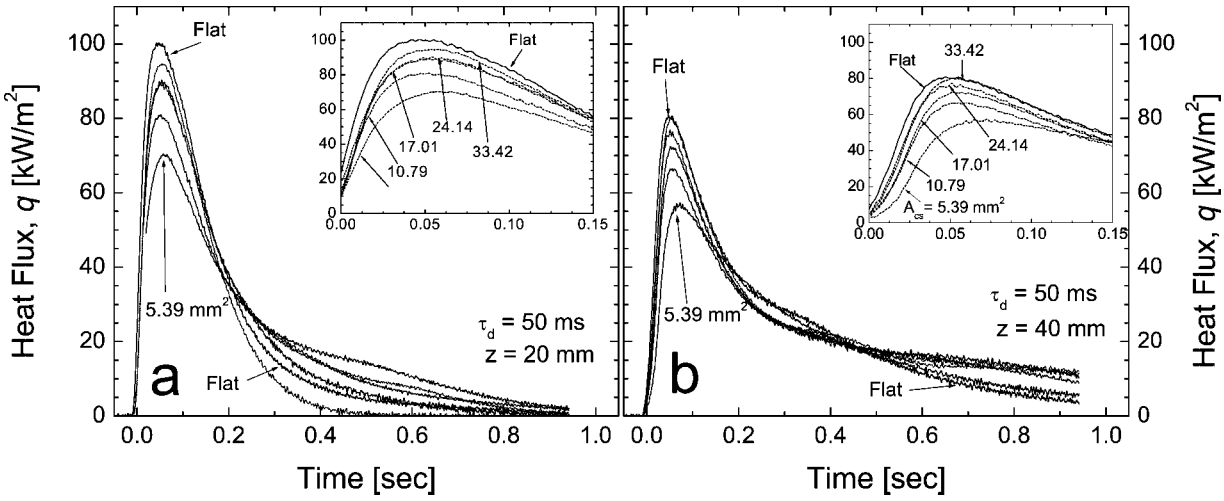

Fig. 8. Surface heat flux during cryogen spray impingement on curved heat flux sensors for $\tau_d = 50$ milliseconds and $z = 20$ mm (**a**) and 40 mm (**b**). The first 150 milliseconds after spurt onset is enlarged in the inset window. In both cases, the flat sensor reaches the highest q_{max} while, amongst the curved sensors, q_{max} increases as A_{cs} increases.

of a thicker liquid layer than would be present on a flat surface. The thickening of the liquid layer reduces the efficiency of heat transfer between the cryogen and skin surface as shown by the higher minimum temperature (Fig. 7a,b) and lower q_{max} (Fig. 8a,b) reached during spray impingement on an indented surface when compared to impingement on a flat surface. Significantly after spurt termination ($t \geq 200$ milliseconds), the q curves corresponding to different indentations cross over with no clear trend (Fig. 8a,b). This is likely an indication of the effect of ambient humidity and frost formation that take place long after cryogen has been deposited and evaporated from the surface [23]. However, the magnitude of q at such times is about three to four times smaller than q_{max}. Therefore, the overall heat extraction, Q, follows the same trend of q_{max}.

One might expect that small indentations (i.e., those with small A_{cs}) would produce small changes in the temperature and heat flux behavior in relation to the flat surface while larger indentations produce more drastic changes. However, Figures 7 and 8 clearly show that minimum temperature decreases and maximum heat flux increases as A_{cs} increases—large indentations improve CSC efficiency more than small ones. In order to determine the cause of this somewhat counterintuitive result, we must consider both elements of A_{cs} (i.e., R_c and d) independently.

An increase in R_c was found to produce a slight increase in q_{max}. Since all cryogen present in a given spray impinges within the indentation, the liquid layer deposited by spurts of equal duration and z must contain the same amount of cryogen. The liquid layer is thicker in indentations with $R_c = 6.34$ mm than for 9.52 mm due solely to the geometry of the indentations. When thicker cryogen liquid layers are present, evaporative cooling is inhibited, which increases the temperature differential between the bottom and top of the liquid layer (because cryogen on the bottom of the layer is warmed by the sensor's surface), further reducing cooling efficiency as found by Verkruysse et al. [11], Aguilar et al. [24], and Pikkula et al. [25].

A stronger positive correlation was found between q_{max} and d. The heat flux behavior associated with indentations between 0 and 0.96 mm is unknown. However, for $d > 0.96$ mm, q_{max} increases linearly with d for both z used in this study, as seen in Figure 9 (note that the slopes of the linear regression are the same for both $z = 20$ and 40 mm).

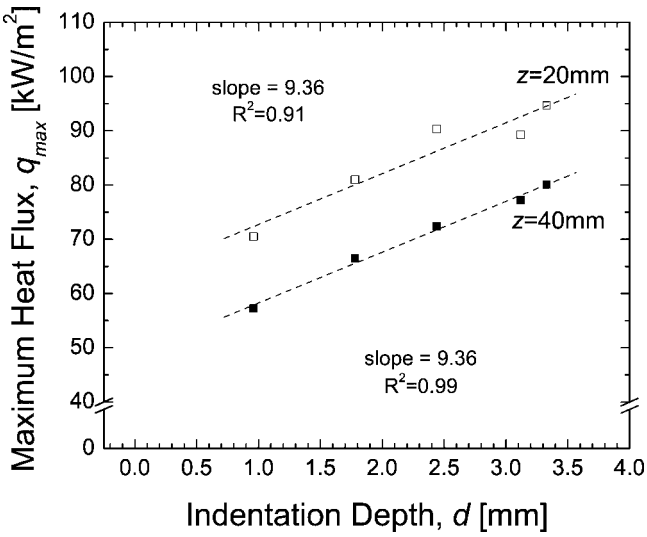

Fig. 9. Variation of maximum heat flux, q_{max}, with depth, d. The behavior of q_{max} between 0 and 0.96 mm is unknown, but q_{max} varies linearly with indentation depth where $d \geq 0.96$ mm. Note that the slope of the linear fit is identical for $z = 20$ and 40 mm.

The maximum indentation made on the sensors was 3.33 mm in depth, which was deeper than any of the indentations measured on the various anatomic locations used for this study which did not exceeded 2.00 mm in depth. However, the linear trend seen here suggests that indentations of even greater depths may provide a better q_{max} than even a flat surface.

Since z was measured from the nozzle tip to the top of the indentation, it must be considered that the true distance over which the cryogen travels ($z_c = z + d$) will change with indentation depth and may contribute to the positive correlation between d and q_{max} noted above. Ongoing work by our group has recently established the dependence of q_{max} on z; correcting z to account for d causes at most a 3–5% decrease in q_{max}. This effect, then, actually causes an underestimation of the positive correlation between d and q_{max} and cannot be used to explain the results of this study.

One possible explanation for the strong positive correlation between q_{max} and d is that indentations of greater depth encourage convective cooling that mitigates the negative effects of liquid layer thickening. In all sprays, the area covered by the cryogen liquid layer expands during spray impingement and some droplets rebound from the surface after initial impact. For very shallow indentations, the cryogen liquid layer expands beyond the indentation edge and droplets are likely to rebound out of the indentation. As d increases, however, the expanding liquid layer is less likely to reach the indentation edge and more likely to recirculate back into the cryogen pool. In addition, the increasing angle of the indented surface makes it more likely that rebounding droplets will fall back into the indentation. Although cryogen from the recirculating liquid layer and any rebounding droplets will slightly thicken the liquid layer, it will also create turbulence and convective flow within the layer. This convective flow improves the heat transfer between the cryogen and sensor surface, mitigating the negative effects of layer thickening and producing a higher maximum heat flux overall.

If this hypothesis is accurate, one would expect cryogen deposits outside shallow indentations but not outside deeper indentations after spray impingement, as layer spreading and droplet rebounding has taken place. A series of high-speed videos were taken of cryogen impingement on indented heat flux sensors of various d using the camera described previously. A frost ring marking the outer limit of the area covered by liquid cryogen is visible in the frames occurring shortly after spurt termination (Fig. 10). For shallow indentations ($d = 1.78$ and 2.44 mm), the frost ring extended beyond the rim of the indentation, suggesting that spreading of the liquid layer and droplet rebound did occur. For $d = 3.12$ mm, however, no frost is ever visible outside the indentation, indicating that any cryogen that otherwise would have exited the indentation has instead been recirculated back into the cryogen pool. This supports the theory of convective flow within the cryogen pool.

CONCLUSIONS

Human skin indents due to the momentum of cryogen spray. A typical spurt used during a dermatological laser treatment can be expected to produce an indentation between 1 and 2 mm in depth. This indentation cause a thicker layer of cryogen to form on the surface, inhibiting heat extraction induced by CSC and reducing the maximum heat flux by as much as 30% when compared to a flat surface. However, increasing indentation depth increases convective heat transfer occurring within the liquid layer, recovering some of the efficiency lost by liquid layer thickening within the indentation. Although eliminating mechanical indentation in the skin entirely would provide the most efficient heat extraction during CSC, reality is that nearly all clinical sprays will induce some indentation. Once indentation exists, one can improve the maximum heat flux and mitigate the effect of cryogen accumulation and liquid layer buildup by physically increasing the size of that indentation. This indicates that nozzles producing higher momentum spurts (and thus greater indentations in the skin) than those currently used may be helpful in improving CSC efficiency and are expected to increase epidermal protection.

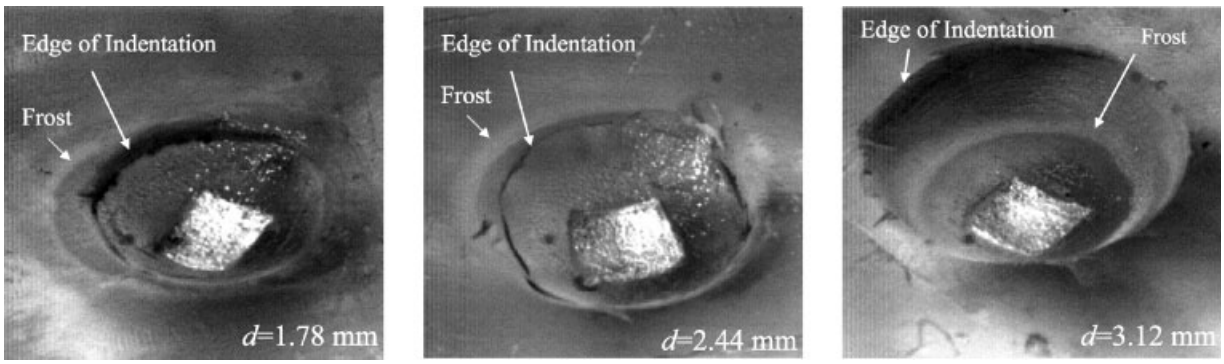

Fig. 10. Photos of pre-deformed sensors after spray impingement. All sensors have $R_c = 6.34$ mm. From **left** to **right**, $d = 1.78$, 2.44, and 3.12 mm. The frost ring indicates the outer perimeter of the cryogen liquid layer following spurt termination. Although all cryogen spray initially impacts within the indentation, the cryogen liquid layer expands beyond the edge of shallow indentations. In deeper indentations, that cryogen does not pass the edge but instead reenters the cryogen pool, causing convective flow, which improves the heat transfer.

ACKNOWLEDGMENTS

Informative discussions with Dr. Bernard Choi, Dr. Sol Kimel, and Dr. Lars Svaasand are greatly appreciated.

REFERENCES

1. Nelson JS, Milner TE, Anvari B, Tanenbaum BS, Kimel S, Svaasand LO, Jacques SL. Dynamic epidermal cooling during pulsed laser treatment of port-wine stain. A new methodology with preliminary clinical evaluation. Arch Dermatol 1995; 131(6):695–700.
2. Altshuler GB, Zenzie HH, Erofeev AV, Smirnov MZ, Anderson RR, Dierickx C. Contact cooling of the skin. Phys Med Biol 1999;44(4):1003–1023.
3. Nelson JS, Majaron B, Kelly KM. What is nonablative photorejuvenation of human skin? Semin Cutan Med Surg 2002;21(4):238–250.
4. Nelson JS, Milner TE, Anvari B, Tanenbaum BS, Svaasand LO, Kimel S. Dynamic epidermal cooling in conjunction with laser-induced photothermolysis of port wine stain blood vessels. Lasers Surg Med 1996;19(2):224–229.
5. Anvari B, Tanenbaum BS, Milner TE, Kimel S, Svaasand LO, Nelson JS. A theoretical study of the thermal response of skin to cryogen spray cooling and pulsed laser irradiation: Implications for treatment of port wine stain birthmarks. Phys Med Biol 1995;40(9):1451–1465.
6. Aguilar G, Majaron B, Verkruysse W, Zhou Y, Nelson JS, Lavernia EJ. Theoretical and experimental analysis of droplet diameter, temperature, and evaporation rate evolution in cryogenic sprays. Int J Heat Mass Tran 2001;44(17): 3201–3211.
7. Anvari B, Ver Steeg BS, Milner TE, Tanebaum BS, Klein TJ, Gerstner E, Kirnel S, Nelson JS. Cryogen spray cooling of human skin: Effects of ambient humidity level, spraying distance, and cryogen boiling point. San Jose, CA: SPIE; 1997. pp 106–110.
8. Aguilar G, Majaron B, Pope K, Svaasand LO, Lavernia EJ, Nelson JS. Influence of nozzle-to-skin distance in cryogen spray cooling for dermatologic laser surgery. Laser Surg Med 2001;28(2):113–120.
9. Aguilar G, Wang GX, Nelson JS. Effect of spurt duration on the heat transfer dynamics during cryogen spray cooling. Phys Med Biol 2003;48(15):2169–2181.
10. Torres JH, Nelson JS, Tanenbaum BS, Milner TE, Goodman DM, Anvari B. Estimation of internal skin temperatures in response to cryogen spray cooling: Implications for laser therapy of port wine stains. IEEE J Sel Top Quant 1999;5(4): 1058–1066.
11. Verkruysse WBM, Aguilar G, Nelson JS, Svaasand LO. Dynamics of cryogen deposition relative to heat extraction rate during cryogen spray cooling. San Jose, CA: SPIE; 2000. pp 37–48.
12. Majaron B, Svaasand LO, Aguilar G, Nelson JS. Intermittent cryogen spray cooling for optimal heat extraction during dermatologic laser treatment. Phys Med Biol 2002;47(18): 3275–3288.
13. Karapetian E, Aguilar G, Kimel S, Lavernia EJ, Nelson JS. Effects of mass flow rate and droplet velocity on surface heat flux during cryogen spray cooling. Phys Med Biol 2003;48(1): N1–N6.
14. Svaasand LO, Randeberg LL, Aguilar G, Majaron B, Kimel S, Lavernia EJ, Nelson JS. Cooling efficiency of cryogen spray during laser therapy of skin. Laser Surg Med 2003;32(2): 137–142.
15. Aguilar G, Verkruysse W, Majaron B, Svaasand LO, Lavernia EJ, Nelson JS. Measurement of heat flux and heat transfer coefficient during continuous cryogen spray cooling for laser dermatologic surgery. IEEE J Sel Top Quant 2001; 7(6):1013–1021.
16. Aguilar G, Wang GX, Nelson JS. Dynamic behavior of cryogen spray cooling: Effects of spurt duration and spray distance. Laser Surg Med 2003;32(2):152–159.
17. Provided by manufacturer. Warwick, RI: RBC industries, Inc.
18. www.matweb.com—visited on 08/02/03.
19. Duck FA. Physical properties of tissue: A comprehensive reference book. London, San Diego: Academic Press; 1990. p 346.
20. Beck JV, Blackwell B, St. Clair CR. Inverse heat conduction: Ill-posed problems. New York, NY: Wiley; 1985.
21. Tunnell JW, Torres JH, Anvari B. Methodology for estimation of time-dependent surface heat flux due to cryogen spray cooling. Ann Biomed Eng 2002;30(1):19–33.
22. Majaron B, Kimel S, Verkruysse W, Aguilar G, Pope R, Svaasand LO, Lavernia EJ, Nelson JS. Cryogen spray cooling in laser dermatology: Effects of ambient humidity and frost formation. Laser Surg Med 2001;28(5):469–476.
23. Aguilar G, Diaz SH, Lavernia EJ, Nelson JS. Cryogen spray cooling efficiency: Improvement of port wine stain laser therapy through muttiple-intermittent cryogen spurts and laser pulses. Laser Surg Med 2002;31(1):27–35.
24. Pikkula BM, Torres JH, Tunnell JW, Anvari B. Cryogen spray cooling: Effects of droplet size and spray density on heat removal. Lasers Surg Med 2001;28(2):103–112.